A Study of Flow and Water Quality in Lake Yanaka

ホアン グアンウェイ, 東京大学,〒113, 文京区本郷 7-3-1 E-mail: huang@hydra.t.u-tokyo.ac.jp
玉井 信行, 東京大学,〒113, 文京区本郷 7-3-1 E-mail: tamai@hydra.t.u-tokyo.ac.jp
アプト ヨハン, (株) 大林組土木技術本部, 〒113, 文京区本郷 2-2-9 センチュリータワー

In this study, numerical simulation and field observation of wind-driven flow pattern in lake Yanaka are carried out. The field observation is made by taking photos from airplane to trace the movements of drifters. It is shown that the simulated flow pattern is in fair agreement with the observation. Subsequently, a compartment model of eutrophication for lake Yanaka is devised to simulate phytoplankton growth. By comparison with field data of 1996, it is shown that the spring bloom in 1996 is well reproduced by the model.

1. Introduction

Lake Yanaka is part of the Watarase retarding basin, north of Tokyo. Its main purpose is three-fold: flood protection, drinking water supply of the Tokyo area and maintenance water for downstream rivers. It has a surface area of 4.5 km^2 and an average depth of six meters with seasonal changes of about three meters for flood control. The lake is divided into three blocks by levees and connected by gaps.

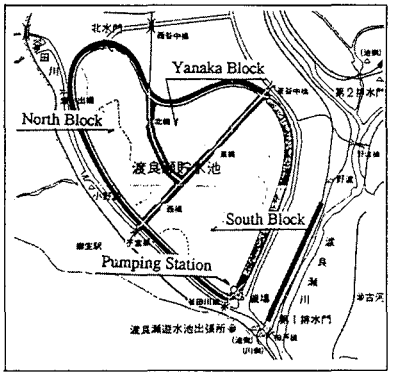

Fig. 1 Lake Yanaka

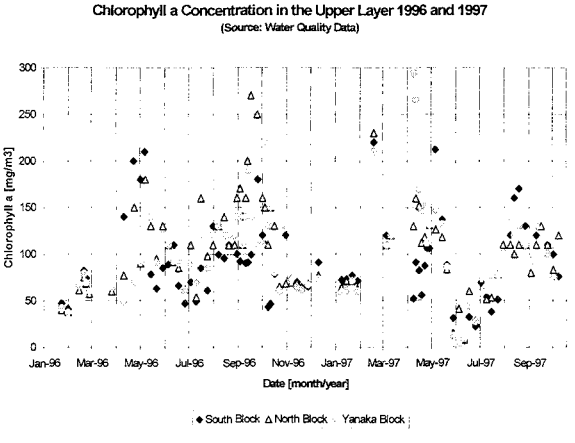

Fig. 2 Concentration of chlorophyll a

In recent years, the eutrophication problem has come up in Lake Yanaka. High inputs of nutrients led to excessive growth of phytoplankton. For example, the concentration of chlorophyll a in Lake Yanaka usually ranges between 50 μg/l and 150 μg/l with peaks of up to more than 250 μg/l as shown in Fig.2. To obtain fundamental understanding in the physical, chemical and biological processes that affect the biomass of phytoplanton in the lake, numerical simulation of wind-driven currents in lake yanaka is performed first, and compared with field measurement carried out last winter. Subsequently, a compartment model of eutrophication is devised for predicting phytoplanton growth in lake Yanaka, and the model output is found to be in fair agreement with measured data.

2. Hydrodynamic model

2.1 Model Description

As shown in Fig.3, Lake Yanaka has a maximum water depth of about 7 m and much lower depths during most time of the year. In addition to that, field data showed that even in spring or summer, the stratification was weak in lake Yanaka. Therefore, in the present study, the two-dimensional depth-averaged shallow water equations were employed which are given below:

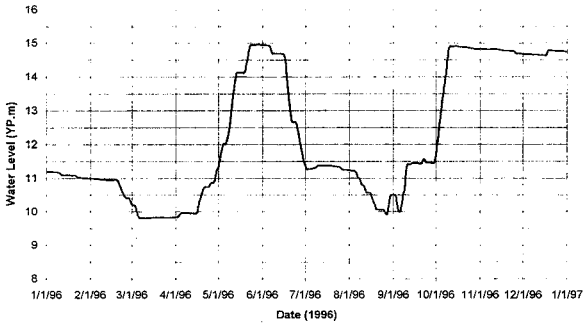

Fig. 3 Variation of water level in lake Yanaka

$$\frac{\partial z}{\partial t}+\frac{\partial (H\cdot U)}{\partial x}+\frac{\partial (H\cdot V)}{\partial y}=0 \tag{1}$$

$$\frac{\partial U}{\partial t}+U\cdot\frac{\partial U}{\partial x}+V\cdot\frac{\partial U}{\partial y}-f\cdot V+g\cdot\frac{\partial h}{\partial x}-\frac{\tau_{SX}-\tau_{BX}}{H\cdot\rho_w}=0 \tag{2}$$

$$\frac{\partial V}{\partial t}+U\cdot\frac{\partial V}{\partial x}+V\cdot\frac{\partial V}{\partial y}+f\cdot U+g\cdot\frac{\partial h}{\partial y}-\frac{\tau_{SY}-\tau_{BY}}{H\cdot\rho_w}=0 \tag{3}$$

H ... water depth

z ... water surface elevation

U, V ... depth averaged velocities

τ_S ... wind shear stress

$\tau_{SX}=\rho_a\cdot c_S\cdot W_X\cdot\sqrt{W_X^2+W_Y^2}$

$\tau_{SY}=\rho_a\cdot c_S\cdot W_Y\cdot\sqrt{W_X^2+W_Y^2}$

W_X, W_Y ... wind velocity in x- and y-direction

c_S ... wind friction coefficient

$c_S=(1+0.07\cdot U_{10})\cdot 10^{-3}$

τ_B ... bottom shear stress using the Manning equation

$\tau_{BX}=\rho_w\frac{g\cdot n^2}{H^{\frac{1}{3}}}\cdot U\cdot\sqrt{V^2+U^2}$

$\tau_{BY}=\rho_w\frac{g\cdot n^2}{H^{\frac{1}{3}}}\cdot V\cdot\sqrt{V^2+U^2}$

n ... Manning's friction coefficient of 0.03

f ... Coriolis coefficient

The equations were discretised with an explicit finite difference method using a central scheme. The grid was staggered in both space and time with a spatial size of 100 m as shown in Fig.4. The physical geometry of the lake was replaced with "zig-zag" approximation in the computation. At the solid boundary, the no-penetration condition was given for velocity, and the initial condition was the calm situation.

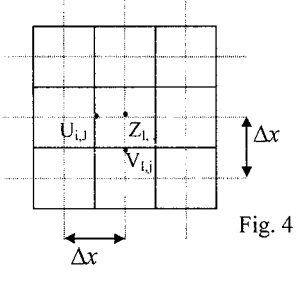

Fig. 4

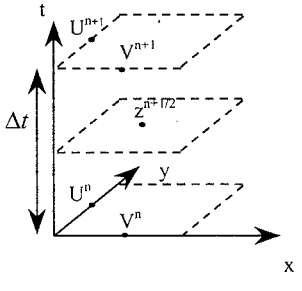

The water surface elevation are calculated at the nodal points in a prediction-correction fashion, while the velocities were calculated at the interfaces of the grid. The numerical algorithm can be written as follows:

Prediction step for surface elevation calculation:

$$\hat{z}_{i,j}^{t+1/2} = z_{i,j}^{t-1/2} - \frac{\Delta t}{2\cdot\Delta x}\Big[U_{i+1,j}\cdot\left(H_{i,j}+H_{i+1,j}\right) - U_{i,j}\cdot\left(H_{i,j}+H_{i-1,j}\right) + V_{i,j+1}\cdot\left(H_{i,j+1}+H_{i,j}\right) - V_{i,j}\cdot\left(H_{i,j}+H_{i,j-1}\right)\Big] \tag{4}$$

Equations of momentum solved at time point n+1:

x-direction:

$$VV = (V_{i,j} + V_{i-1,j} + V_{i,j+1} + V_{i-1,j+1})\cdot\frac{1}{4} \tag{5}$$

$$H_{mx} = (H_{i,j} + H_{i-1,j})\cdot\frac{1}{2} \tag{6}$$

or, if the water surface elevation shall be taken into account H would be replaced by h.

$$AD = \frac{(U_{i,j}+U_{i+1,j})^2 - (U_{i,j}+U_{i-1,j})^2}{8\Delta x} + \frac{VV\cdot(U_{i,j+1}-U_{i,j-1})}{2\Delta x} \tag{7}$$

$$UN_{i,j} = U_{i,j} - \Delta t\cdot\left[AD + \frac{g\cdot(\hat{z}_{i,j}-\hat{z}_{i-1,j})}{\Delta x} + f\cdot VV - \frac{(\tau_{SX}-\tau_{BX})}{H_{mx}}\right] \tag{8}$$

y-direction:

$$UU = (U_{i,j} + U_{i+1,j} + U_{i,j-1} + U_{i+1,j-1})\cdot\frac{1}{4} \tag{9}$$

$$H_{my} = (H_{i,j} + H_{i,j-1})\cdot\frac{1}{2} \tag{10}$$

$$AD = \frac{(V_{i,j+1}+V_{i,j})^2 - (V_{i+1,j}+V_{i,j-1})^2}{8\Delta x} + \frac{UU\cdot(V_{i+1,j}-V_{i-1,j})}{2\Delta x} \tag{11}$$

$$VN_{i,j} = V_{i,j} - \Delta t\cdot\left[AD + \frac{g\cdot(\hat{z}_{i,j}-\hat{z}_{i,j-1})}{\Delta x} + f\cdot UU - \frac{(\tau_{SY}-\tau_{BY})}{H_{my}}\right] \tag{12}$$

Correction step for surface elevation calculation:

$$z_{i,j}^{t+1/2} = \frac{1}{2}\hat{z}_{i,j}^{t+1/2} + \frac{1}{2}\{z_{i,j}^{t-1/2} - \frac{\Delta t}{2\cdot\Delta x}\Big[UN_{i+1,j}\cdot\left(H_{i,j}+H_{i+1,j}\right) - U_{i,j}N\cdot\left(H_{i,j}+H_{i-1,j}\right) + VN_{i,j+1}\cdot\left(H_{i,j+1}+H_{i,j}\right) - VN_{i,j}\cdot\left(H_{i,j}+H_{i,j-1}\right)\Big]\} \tag{13}$$

2.2 Characteristics of the Wind Field over Lake Yanaka

Figure 5(a) shows the variation of the observed wind directions in 1996. As can be seen, prevailing wind directions were from north-east, west-north-west and east-south-eastern directions. 80 % of the magnitudes of hourly averaged wind speed ranged from 1 to 6 m/s. Fig.5(b) shows that during the winter of 1996, WNW was the dominant direction for wind speed higher than 4 m/s. The meteorological observation station is located near the pumping station of the lake. In order to obtain wind data for running the hydrodynamic model, field measurement of wind over lake Yanaka was carried out from November 28th to December 5th, 1997, in addition to the flow pattern observation. The time variation of wind speed (m/s) and its direction during that period is presented in Fig. 5.

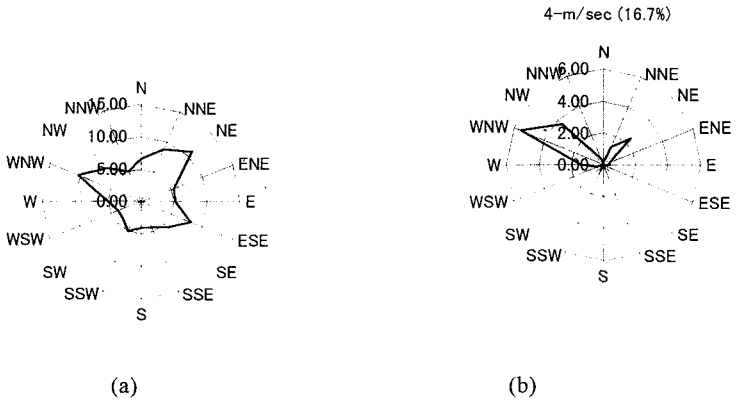

(a) (b)

Fig. 5 Wind Rose over Lake Yanaka

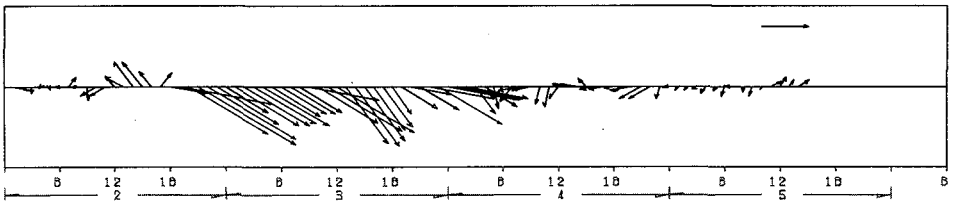

Fig.6 Wind field between Dec. 2nd and 5th, 1997

2.3 Flow Pattern Observation

For the investigation on the circulation patterns in lake Yanaka, a number of drifters were released into the lake. Drifters consisted of a cross vane suspended by a nylon cord and a float. The actual depths of the cross vane varied depending on the flow depth where observation was aimed at. The drifters were designed after Bhowmik and Stall (1978), who tested the cross-vane movement with the average velocity of the surrounding water in a flume and described the correlation to be "excellent". Modification was necessary for the float, which had to be at least 50 cm in diameter in the horizontal plane to be recognized on photographs taken from airplane. After the drifters were released into the lake, photographs were taken hourly from an airplane at a height of approximately 700m. By applying aerial photo processing technique, the movements of drifters were traced.

2.4 Comparison of Numerical Results with Field Observation

With the wind speed and direction taken from the measured data, Fig. 6 shows the simulated flow pattern at 11:00 Dec. 4th, 1997. It is clear that a big swirl forms in South Block, and a relative small circulation is predicted in North Block near the opening between South and North Block. The observed flow pattern is given in Fig.7. As can be seen, the computed flow pattern is in fair agreement with observed. The sensitivity analysis indicated that the Coriolis force exerts almost no effect on the flow pattern in Lake Yanaka, which can also be realised if one pays attention to the largeness of Rossby number for Lake Yanaka.

3. Eutrophication Model and Output

Field measurements of water quality in lake Yanaka were carried out last summer and winter. The multi-point measurement data indicated that the variations of water quality index such as water temperature, DO, pH, and turbidity within each block of lake Yanaka are quite small. Therefore, by assuming well-mixedness in each block, a compartment model was developed consisting of three interconnected compartments, namely South Block, North Block and Yanaka Block. Another assumption involved in the model is that phosphorus is the limiting nutrient for the growth of phytoplankton in lake Yanaka. The modelled state variables considered in phosphorus cycle were inorganic orthophosphate, organic phosphorus and internal phosphorus which were simulated to represent the phosphorus cycle as well as phytoplankton modeled as chlorophyll a. Other parameters were given as input. The model was linked to the hydrodynamic model by estimating interflow due to wind by the hydrodynamic model.

The phytoplankton kinetics can be written schematically and as differential equations as:
Change Rate = + Growth – Respiration – Mortality – Zooplankton Grazing
– Deposition

$$\frac{\partial Phyt}{\partial t} = \left\{ G_P \cdot Min\left(\frac{f_{dissPO_4P} \cdot PO_4P}{K_P + f_{dissPO_4P} \cdot PO_4P}; \frac{NO_3 + NH_4}{K_N + NO_3 + NH_4}; f(I) \right) - k_r - k_m \right\} \cdot f_p(T) \cdot Phyt$$

$$- k_{gz} \cdot f_{gz}(T) \cdot f_{gz}(P) \cdot Z \cdot Phyt - \frac{v_{SPhyt}}{h} \cdot Phyt$$

$$f(I) = \frac{2.1781}{K_e \cdot h} \cdot f \cdot \left[\exp\left\{ -\frac{I_a}{I_S} \cdot \exp(-K_e \cdot h) \right\} - \exp\left(-\frac{I_a}{I_S} \right) \right]$$

$$K_{eshd} = 0.0088 \cdot Chla + 0.054 \cdot Chla^{0.667}$$

$$f_P(T) = \vartheta_P^{T-20}\ ;\ f_{gz}(T) = \vartheta_{gz}^{T-20};\ f_{gz}(P) = \frac{Phyt}{K_{PZ} + Phyt}$$

Nitrate and ammonia concentrations were given as input in the present study. Growth rate was a function of nutrient supply, light, and temperature in this model. In principle the phytoplankton growth rate can be expressed either in terms of the external concentration of the limiting nutrient (Monod model) or as a function of the internal nutrient concentration (cell quota) of the limiting nutrient (Droop model). This model applied the Monod growth kinetics where growth is a direct function of the nutrient concentration in water. It was assumed that at an adequate level of substrate concentration the growth rate proceeds at the saturated rate for the ambient temperature conditions present. At low substrate concentration however, the growth rate becomes linearly proportional to substrate concentration. Thus, for a nutrient with concentration N, the factor by which the saturated growth rate is reduced is $N/(K_m + N)$. The constant K_m is called the Michaelis or half-saturation constant. It is the nutrient concentration at which the growth rate is half the saturated growth rate. Temperature dependence was determined from the work of Eppley (1972) referenced by Thomann and Mueller (1987, p. 419) as $f_P(T) = \vartheta_P^{T-20}$. The effect of light limitation followed the approach of Ambrose et al..

Phytoplankton loss terms included respiration (including excretion), natural mortality and zooplankton grazing. The terms for respiration and mortality were modeled in the usual manner as first order losses, with an identical temperature dependence to that for growth (Hamilton and Schladow, 1997). Zooplankton grazing was modeled by a Monod function, varying with season, chlorophyll a concentration, and temperature. Biomass of zooplankton was not modeled explicitly.

Gravitational settling of phytoplankton was an important contribution to the overall mortality of the phytoplankton population. The settling velocity of phytoplankton under laboratory and real conditions has been reported to vary widely from 0.07 m/day to 18 m/day and even zero or negative velocities may occur (Ambrose et al.). Actual settling in natural waters is a complex phenomenon affected by vertical turbulence, density gradients, and the physiological state of the different species. In this model the settling velocity was defined as a function of water depth and wind speed. Higher wind speeds and little water depth increase the turbulent mixing in the lake while the settling velocity during calm seasons and high water levels was expected to be higher. The model has been run repeatedly for parameter adjusting.

The simulated chlorophyll a concentration in three blocks for 1996 are presented in Fig.8, together with the filed data for the purpose of comparison. It can been seen that the peak of the chlorophyll a concentration in the middle of April , 1996 was well captured. Also the sharp decrease after reaching the peak seems to be reasonably modelled.

4. Concluding Remark

The conclusions of the present study are given as following:

- Numerical analysis of wind-generated flow pattern in lake Yanaka is performed with a 2-D model, and compared qualitatively well with the field observation. The results suggest that a large circulation may form in the South Block of the lake.
- A three-compartment eutrophication model was designed to compute phytoplankton growth, and the model output shows that the model is plausible.

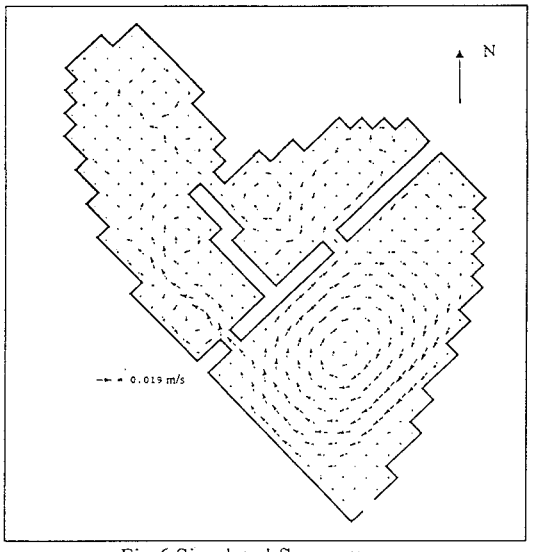

Fig.6 Simulated flow pattern

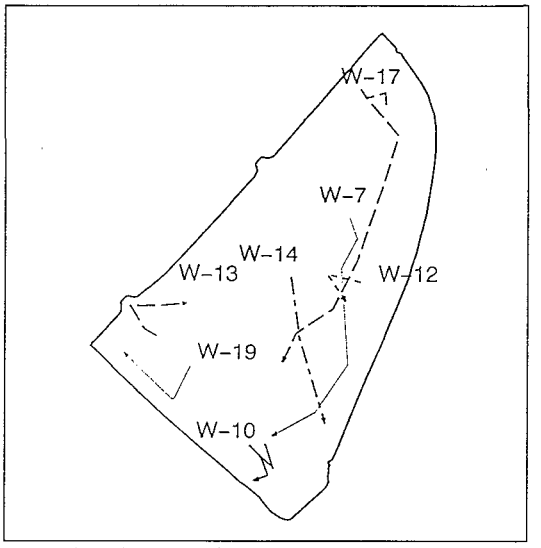

Fig.7 Observed flow pattern in South Block

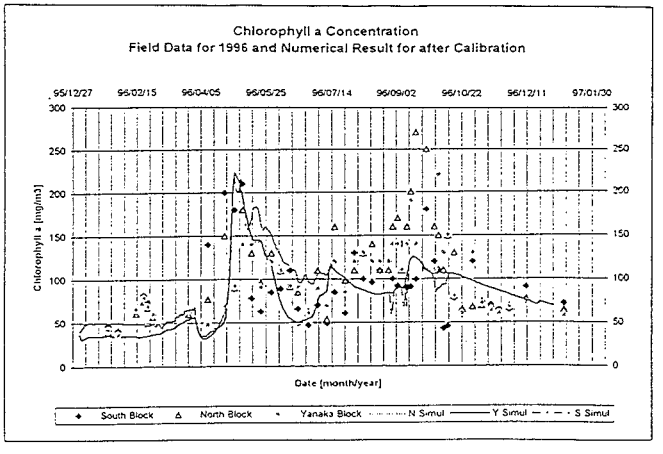

Fig. 8 Comparison of predicted chlorophyll a concentration with measured data

Acknowledgement

The first author would like to express his gratitude to Dr. Kawahara and Mr. Matsuzaki for their valuable suggestions. And thanks should also be given to the Upper Tone River Construction Office for their kind assistance in field observation and data collection.

References

1. Weiyan, Tan, "Shallow Water Hydrodynamics", Amsterdam, Elsevier, 1992.
2. Fischer Hugo B., "Transport Models for Inland and Coastal Waters", 1981.
3. Ambrose, R.B., "Modeling volatile organics in the Delaware estuary", J. of Environmental Engineering, V. 113, No.4, 703-721, 1987.
4. Biermann Jr, V.J., D.M. Dillon, "Modeling of phytoplankton in Saginaw Bay: II. Post-Audit-Phase", ASCE, J. of Environmetal Engineering, 112, 400-414, 1986.
5. Carrick, H.K., F.J., Aldridge, "Wind influences phytoplankton biomass and composition in a shallow, productive lake", Limnol. Oceanogr., 38, 1179-1192, 1993.